Mesoscopic fluctuations of the Loschmidt echo

Cyril Petitjean and Philippe Jacquod
Département de Physique Théorique, Université de Genève, CH-1211 Genève 4, Switzerland

(Received 13 October 2004; revised manuscript received 31 January 2005; published 29 March 2005)

We investigate the time-dependent variance of the fidelity with which an initial narrow wave packet is reconstructed after its dynamics is time reversed with a perturbed Hamiltonian. In the semiclassical regime of perturbation, we show that the variance first rises algebraically up to a critical time t_c, after which it decays. To leading order in the effective Planck's constant $\hbar_{\rm eff}$, this decay is given by the sum of a classical term $\simeq \exp[-2\lambda t]$, a quantum term $\simeq 2\hbar_{\rm eff}\exp[-\Gamma t]$, and a mixed term $\simeq 2\ \exp[-(\Gamma+\lambda)t]$. Compared to the behavior of the average fidelity, this allows for the extraction of the classical Lyapunov exponent λ in a larger parameter range. Our results are confirmed by numerical simulations.

DOI: 10.1103/PhysRevE.71.036223 PACS number(s): 05.45.Mt, 74.40.+k, 03.65.Yz

The fluctuations of a physical quantity often contain more information than its average. For example, quantum signatures of classical chaos are absent of the average density of states, but strongly affect spectral fluctuations [1]. In the search for such signatures, another approach has been to investigate the sensitivity to an external perturbation that is exhibited by the quantum dynamics [2]. Going back to Ref. [3], the central quantity in this approach is the Loschmidt echo [4], the fidelity

$$M(t) = |\langle \psi_0 | \exp[iHt]\exp[-iH_0 t]|\psi_0\rangle|^2 \qquad (1)$$

with which an initial quantum state ψ_0 is reconstructed after the dynamics is time reversed using a perturbed Hamiltonian, $H = H_0 + \epsilon V$ (we set $\hbar \equiv 1$). This approach proved very fruitful; however, most investigations of $M(t)$ (which we will briefly summarize below) considered the properties of the *average* fidelity $\overline{M(t)}$, either over different ψ_0, or different elements of an ensemble of unperturbed Hamiltonians H_0 (having, for instance, the same classical Lyapunov exponent λ) and/or perturbation V. Curiously enough, the variance $\sigma^2(M)$ of the fidelity has been largely neglected so far. The purpose of this paper is to fill this gap. We will see that the variance $\sigma^2(M)$ has a much richer behavior than $\overline{M(t)}$, allowing for the extraction of λ in a larger parameter range, and exhibiting a nonmonotonous behavior with a non-self-averaging maximal value $\sigma(t_c)/\overline{M(t_c)} \simeq 1$.

We first summarize what is known about the average fidelity $\overline{M(t)}$ in quantum chaotic systems. Three regimes of perturbation strength are differentiated by three energy scales [5]: the energy bandwidth B of H_0, the golden rule spreading $\Gamma = 2\pi\epsilon^2 \overline{|\langle \phi_\alpha^{(0)}|V|\phi_\beta^{(0)}\rangle|^2}/\Delta$ of an eigenstate $\phi_\alpha^{(0)}$ of H_0 over the eigenbasis $\{\phi_\alpha\}$ of H, and the level spacing $\Delta = B\hbar_{\rm eff}$ ($\hbar_{\rm eff} = \nu^d/\Omega$ is the effective Planck's constant, given by the ratio of the wavelength volume to the system's volume). These three regimes are: (i) the weak perturbation regime $\Gamma < \Delta$, with a typical Gaussian decay $\overline{M(t)} \simeq \exp(-\overline{\Sigma^2}t^2)$, $\Sigma^2 \equiv \epsilon^2(\langle\psi_0|V^2|\psi_0\rangle - \langle\psi_0|V|\psi_0\rangle^2)$, $\overline{\Sigma^2} \simeq \Gamma\Delta\hbar_{\rm eff}^{-1}$ [3,6] (corrections to this Gaussian decay have been discussed in Ref. [7]); (ii) the semiclassical golden rule regime $\Delta < \Gamma < B$, where the decay is exponential with a rate set by the smallest of Γ and λ, $\overline{M(t)} \simeq \exp[-\min(\Gamma,\lambda)t]$ [4,5,8]; and (iii) the strong perturbation regime $\Gamma > B$ with another Gaussian decay $\overline{M(t)} \simeq \exp(-B^2t^2)$ [5]. This classification is based on the scheme of Ref. [5], which relates the behavior of $\overline{M(t)}$ to the local spectral density of eigenstates of H_0 over the eigenbasis of H [5,9]. Accordingly, regime (ii) corresponds to the range of validity of Fermi's golden rule, where the local spectral density has a Lorentzian shape [5,9,10]. Quantum disordered systems with diffractive impurities, on the other hand, have been predicted to exhibit golden rule decay $\propto \exp[-\Gamma t]$ and Lyapunov decay $\propto \exp[-\lambda t]$ in different time intervals for a single set of parameters [12]. It is also worth mentioning that regular systems exhibit a very different behavior, where in the semiclassical regime (ii), $\overline{M(t)}$ decays as a power law [13] (see also Ref. [14]). Finally, while in chaotic systems the averaging procedure has been found to be ergodic, i.e., considering different states ψ_0 is equivalent to considering different realizations of H_0 or V, the Lyapunov decay exists only for specific choices where ψ_0 has a well-defined classical meaning, like a coherent or a position state [4,11,15,16].

Investigations beyond this qualitative picture have focused on crossover regions between the regimes (i) and (ii) [7] and deviations from the behavior (ii) $\simeq \exp[-\min(\Gamma,\lambda)t]$ due to action correlations in weakly chaotic systems [17]. Reference [18] provides the only analytical investigation of the fluctuations of $M(t)$ to date. It shows that, for classically large perturbations, $\Gamma \gg B$, $\overline{M(t)}$ is dominated by very few exceptional events, so that a typical ψ_0's fidelity is better described by $\exp[\overline{\ln(M)}]$, and that $M(t)$ does not fluctuate after the Ehrenfest time $t_E = \lambda^{-1}|\ln[\hbar_{\rm eff}]|$. We will see that these conclusions do not apply to the regime (ii) of present interest. While some numerical data for the distribution of $M(t)$ in the weak perturbation regime (i) were presented in Ref. [19], we focus here on chaotic systems and investigate the behavior of $\sigma^2(M)$ in the semiclassical regime (ii).

We first follow a semiclassical approach along the lines of Ref. [4]. We consider an initial Gaussian wave packet $\psi_0(\mathbf{r}_0') = (\pi\nu^2)^{-d/4}\exp[i\mathbf{p}_0\cdot(\mathbf{r}_0'-\mathbf{r}_0) - |\mathbf{r}_0'-\mathbf{r}_0|^2/2\nu^2]$, and approximate its time evolution by

$$\langle \mathbf{r}|\exp(-iH_0t)|\psi_0\rangle = \int d\mathbf{r}_0' \sum_s K_s^{H_0}(\mathbf{r},\mathbf{r}_0';t)\psi_0(\mathbf{r}_0'),$$

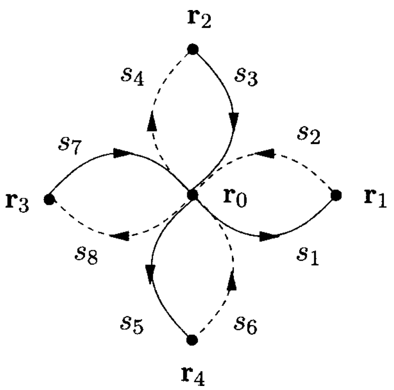

FIG. 1. Diagrammatic representation of the squared fidelity $M^2(t)$.

$$K_s^{H_0}(\mathbf{r},\mathbf{r}_0';t) = \frac{C_s^{1/2}}{(2\pi i)^{d/2}}\exp[iS_s^{H_0}(\mathbf{r},\mathbf{r}_0';t) - i\pi\mu_s/2]. \quad (2)$$

The semiclassical propagator is expressed as a sum over classical trajectories (labeled s) connecting $\mathbf{r}$ and $\mathbf{r}_0'$ in the time t. For each s, the partial propagator contains the action integral $S_s^H(\mathbf{r},\mathbf{r}_0';t)$ along s, a Maslov index μ_s, and the determinant C_s of the stability matrix [21]. We recall that this approach allows us to calculate the time evolution of smooth, localized wave packets up to algebraically long times $\propto O(\hbar_{\text{eff}}^{-a}) \gg t_E$ (with $a>0$) [22].

The fidelity then reads,

$$M(t) = \left| \int d\mathbf{r}_1 \int d\mathbf{r}_0' \int d\mathbf{r}_0'' \psi_0(\mathbf{r}_0')\psi_0^*(\mathbf{r}_0'') \times \sum_{s_1,s_2} K_{s_1}^{H_0}(\mathbf{r}_1,\mathbf{r}_0';t)[K_{s_2}^{H}(\mathbf{r}_1,\mathbf{r}_0'';t)]^* \right|^2. \quad (3)$$

We want to calculate $M^2(t)$. Squaring Eq. (3), we see that $M^2(t)$ is given by eight sums over classical paths and 12 spatial integrations. Noting that ψ_0 is a narrow Gaussian wave packet, we first linearize all eight action integrals around $\mathbf{r}_0$,

$$S_s(\mathbf{r},\mathbf{r}_0';t) \simeq S_s(\mathbf{r},\mathbf{r}_0;t) - (\mathbf{r}_0' - \mathbf{r}_0)\cdot\mathbf{p}_s. \quad (4)$$

We can then perform the Gaussian integrations over the eight initial positions $\mathbf{r}_0'$, $\mathbf{r}_0''$, and so forth. In this way $M^2(t)$ is expressed as a sum over eight trajectories connecting $\mathbf{r}_0$ to four independent final points $\mathbf{r}_j$ over which one integrates,

$$M^2(t) = \int \prod_{j=1}^{4} d\mathbf{r}_j \sum_{s_i;i=1}^{8} \exp[i(\Phi^{H_0} - \Phi^H - \pi\mathcal{M}/2)] \times \left[\prod_i C_{s_i}^{1/2}\left(\frac{\nu^2}{\pi}\right)^{d/4}\exp(-\nu^2\delta\mathbf{p}_{s_i}^2/2)\right], \quad (5)$$

where we introduced $\mathcal{M}=\Sigma_{i=0}^{3}(-1)^i(\mu_{s_{2i+1}}-\mu_{s_{2i+2}})$ and $\delta\mathbf{p}_{s_i}=\mathbf{p}_{s_i}-\mathbf{p}_0$.

The expression of Eq. (5) is schematically described in Fig. 1. Classical trajectories are represented by a full line if they correspond to H_0 and a dashed line for H, with an arrow indicating the direction of propagation. In the semiclassical limit $S_s \gg 1$ (we recall that actions are expressed in units of $\hbar$), Eq. (5) is dominated by terms that satisfy a stationary phase condition, i.e., where the variation of the difference of the two action phases

$$\Phi^{H_0} = S_{s_1}^{H_0}(\mathbf{r}_1,\mathbf{r}_0;t) - S_{s_3}^{H_0}(\mathbf{r}_0,\mathbf{r}_2;t) + S_{s_5}^{H_0}(\mathbf{r}_4,\mathbf{r}_0;t) - S_{s_7}^{H_0}(\mathbf{r}_0,\mathbf{r}_3;t), \quad (6a)$$

$$\Phi^{H} = S_{s_2}^{H}(\mathbf{r}_0,\mathbf{r}_1;t) - S_{s_4}^{H}(\mathbf{r}_2,\mathbf{r}_0;t) + S_{s_6}^{H}(\mathbf{r}_0,\mathbf{r}_4;t) - S_{s_8}^{H}(\mathbf{r}_3,\mathbf{r}_0;t), \quad (6b)$$

has to be minimized. These stationary phase terms are easily identified from the diagrammatic representation as those where two classical trajectories s and s' of opposite direction of propagation are *contracted*, i.e., $s=s'$, up to a quantum resolution given by the wavelength ν [23]. This is represented in Fig. 2 by bringing two lines together in parallel. Contracting either two dashed or two full lines allows for an almost exact cancellation of the actions, hence an almost perturbation-independent contribution, up to a contribution arising from the finite resolution ν with which the two paths overlap. However when a full line is contracted with a dashed line, the resulting contribution still depends on the action $\delta S_s=-\epsilon\int_s V(\mathbf{q}(t),t)$ accumulated by the perturbation along the classical path s, spatially parametrized as $\mathbf{q}(t)$. Since we are interested in the variance $\sigma^2(M)=\overline{M^2}-\overline{M}^2$ (this is indicated by brackets in Fig. 2), we must subtract the terms contained in $\overline{M}^2$ corresponding to independent contractions in each of the two subsets (s_1,s_2,s_3,s_4) and (s_5,s_6,s_7,s_8). Consequently, all contributions to $\sigma^2(M)$ require pairing of spatial coordinates, $|\mathbf{r}_i-\mathbf{r}_j|\leq\nu$, for at least one pair of indices $i,j=1,2,3,4$.

With these considerations, the four dominant contributions to $\sigma^2(M)$ are depicted on the right-hand side of Fig. 2. The first one corresponds to $s_1=s_2\simeq s_7=s_8$ and $s_3=s_4\simeq s_5=s_6$, which requires $\mathbf{r}_1\simeq\mathbf{r}_3$, $\mathbf{r}_2\simeq\mathbf{r}_4$. This gives a contribution

$$\sigma_1^2 = \left(\frac{\nu^2}{\pi}\right)^{2d}\left\langle \int d\mathbf{r}_1 d\mathbf{r}_3 \sum C_{s_1}^2 \times \exp[-2\nu^2\delta\mathbf{p}_{s_1}^2 + i\delta\Phi_{s_1}]\Theta(\nu - |\mathbf{r}_1-\mathbf{r}_3|)\right\rangle^2, \quad (7)$$

where $\delta\Phi_{s_1}=\epsilon\int_0^t dt'\nabla V(\mathbf{q}(t'))[\mathbf{q}_{s_1}(t')-\mathbf{q}_{s_7}(t')]$ arises from the linearization of V on $s=s_{1,2}\simeq s'=s_{7,8}$ [4,11], and $\mathbf{q}_{s_1}(\tilde{t})$ lies on s_1 with $\mathbf{q}(0)=\mathbf{r}_0$ and $\mathbf{q}(t)=\mathbf{r}_1$. In Eq. (7) the integrations are restricted by $|\mathbf{r}_1-\mathbf{r}_3|\leq\nu$ because of the finite resolution with which two paths can be equated (this is also enforced by the presence of $\delta\Phi_s$ as we will see momentarily). For long enough times, $t\gg t^*$, the phases $\delta\Phi_s$ fluctuate randomly and exhibit no correlation between different trajectories [20]. One thus applies the central limit theorem (CLT) $\langle\exp[i\delta\Phi_s]\rangle=\exp[-\langle\delta\Phi_s^2\rangle/2]\simeq\exp[-\epsilon^2\int dt\langle\nabla V(0)\cdot\nabla V(t)\rangle|\mathbf{r}_1-\mathbf{r}_3|^2/2\lambda]$. After performing a change of integration variable $\int d\mathbf{r}\Sigma_s C_s=\int d\mathbf{p}$ and using the asymptotic expression $C_s\simeq(m/t)^d\exp[-\lambda t]$ [21], one gets

$$\sigma_1^2 = \alpha^2\exp[-2\lambda t], \quad (8a)$$

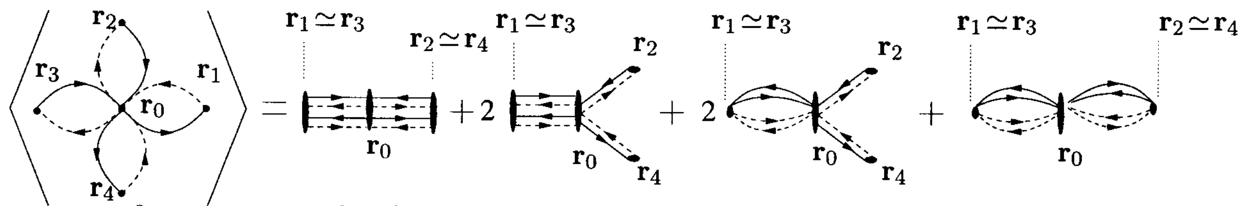

$$\sigma^2(M) = \alpha^2 e^{-2\lambda t} + 2\alpha e^{-\lambda t} e^{-\Gamma t} + 2\hbar_{\rm eff} e^{-\Gamma t}\Theta(t-t_E) + \hbar_{\rm eff}^2 \Theta(t-t_E)$$

FIG. 2. Diagrammatic representation of the averaged fidelity variance $\sigma^2(M)$ and the three time-dependent contributions that dominate semiclassically, together with the contribution giving the long-time saturation of $\sigma^2(M)$.

$$\alpha = \left(\frac{\lambda \nu^2 m^2}{\epsilon^2 t^2 \int d\tau \langle \nabla V(0) \cdot \nabla V(\tau) \rangle} \right)^{d/2}. \tag{8b}$$

The second dominant term is obtained from $s_1 = s_2 \simeq s_7 = s_8$, $s_3 = s_4$ and $s_5 = s_6$, with $\mathbf{r}_1 \simeq \mathbf{r}_3$, or equivalently $s_1 = s_2$, $s_7 = s_8$ and $s_3 = s_4 \simeq s_5 = s_6$ with $\mathbf{r}_2 \simeq \mathbf{r}_4$. Therefore this term comes with a multiplicity of two, and one obtains

$$\sigma_2^2 = 2\left(\frac{\nu^2}{\pi}\right)^{2d} \left\langle \int d\mathbf{r}_1 d\mathbf{r}_3 \sum C_{s_1}^2 \times \exp[-2\nu^2 \delta \mathbf{p}_{s_1}^2 + i\delta\Phi_{s_1}]\Theta(\nu - |\mathbf{r}_1 - \mathbf{r}_3|) \right\rangle \times \left\langle \int d\mathbf{r}_2 \sum C_{s_3} \exp[-\nu^2 \delta \mathbf{p}_{s_3}^2 + i\delta S_{s_3}] \right\rangle^2, \tag{9}$$

again with the restriction $|\mathbf{r}_1 - \mathbf{r}_3| \leqslant \nu$. To calculate the first bracket on the right-hand side of Eq. (9), we first average the complex exponential, assuming again that enough time has elapsed so that actions are randomized. The CLT gives $\langle \exp[i\delta S_{s_3}]\rangle = \exp\left(-\frac{1}{2}\langle \delta S_{s_3}^2\rangle\right)$ with

$$\langle \delta S_{s_3}^2 \rangle = \epsilon^2 \int_0^t d\tilde{t} \int_0^t d\tilde{t}' \langle V[\mathbf{q}(\tilde{t})] V[\mathbf{q}(\tilde{t}')]\rangle. \tag{10}$$

Here $\mathbf{q}(\tilde{t})$ lies on s_3 with $\mathbf{q}(0) = \mathbf{r}_0$ and $\mathbf{q}(t) = \mathbf{r}_2$. In hyperbolic systems, correlators typically decay exponentially fast,

$$\langle V[\mathbf{q}(\tilde{t})] V[\mathbf{q}(\tilde{t}')]\rangle \propto \exp[-\eta |t - t'|], \tag{11}$$

with an upper bound on η set by the smallest positive Lyapunov exponent [24]. One thus obtains $\langle \delta S_{s_3}^2 \rangle = \Gamma t$. Usually $\Gamma \propto \epsilon^2$ is identified with the golden rule spreading of eigenstates of H over those of H_0 [5,7]. It is dominated by the short-time behavior of $\langle V[\mathbf{q}(\tilde{t})] V[\mathbf{q}(0)]\rangle$. We stress however that for long enough times, $\langle \delta S_{s_3}^2 \rangle \propto t$ still holds to leading order even with a power-law decay of the correlator $\langle V[\mathbf{q}(\tilde{t})] V[\mathbf{q}(\tilde{t}')]\rangle \propto |t - t'|^{-\eta}$, provided η is sufficiently large, $\eta \geqslant 1$. We note that similar expressions such as Eq. (10), relating the decay of $\overline{M}$ to time integrations over the perturbation correlator, have been derived in Refs. [6,19] using a different approach than the semiclassical method of Ref. [4] used here. Further, using the sum rule

$$(\nu^2/\pi)^d \left(\int d\mathbf{r} \sum C_s \exp[-\nu^2 \delta \mathbf{p}_s^2] \right)^2 = 1, \tag{12}$$

one finally obtains

$$\sigma_2^2 = 2\alpha \exp[-\lambda t] \exp[-\Gamma t]. \tag{13}$$

The third and last dominant time-dependent term arises from either $s_1 = s_7$, $s_2 = s_8$, $s_3 = s_4$, $s_5 = s_6$, and $\mathbf{r}_1 \simeq \mathbf{r}_3$, or $s_1 = s_2$, $s_3 = s_5$, $s_4 = s_6$, $s_7 = s_8$, and $\mathbf{r}_2 \simeq \mathbf{r}_4$. It thus also has a multiplicity of two and reads

$$\sigma_3^2 = 2\left(\frac{\nu^2}{\pi}\right)^{2d} \left\langle \int d\mathbf{r}_1 d\mathbf{r}_2 d\mathbf{r}_3 d\mathbf{r}_4 \sum C_{s_1} C_{s_2} C_{s_3} C_{s_5} \times \exp[-\nu^2(\delta \mathbf{p}_{s_1}^2 + \delta \mathbf{p}_{s_2}^2 + \delta \mathbf{p}_{s_3}^2 + \delta \mathbf{p}_{s_5}^2)] \times \exp[i(\delta S_{s_3} - \delta S_{s_5})]\Theta(\nu - |\mathbf{r}_1 - \mathbf{r}_3|) \right\rangle. \tag{14}$$

The integrations, again, have to be performed with $|\mathbf{r}_1 - \mathbf{r}_3| \leqslant \nu$. We incorporate this restriction in the calculation by making the ergodicity assumption, i.e. setting,

$$\left\langle \int d\mathbf{r}_1 d\mathbf{r}_2 d\mathbf{r}_3 d\mathbf{r}_4 \ldots \Theta(\nu - |\mathbf{r}_1 - \mathbf{r}_3|) \right\rangle = \hbar_{\rm eff} \left\langle \int d\mathbf{r}_1 d\mathbf{r}_2 d\mathbf{r}_3 d\mathbf{r}_4 \ldots \right\rangle \Theta(t - t_E), \tag{15}$$

which is valid for times larger than the Ehrenfest time [25] (for shorter times, $t < t_E$, the third diagram on the right-hand side of Fig. 2 goes into the second one). One then averages the phases using the CLT to get

$$\sigma_3^2 = 2\hbar_{\rm eff} \exp[-\Gamma t]\Theta(t - t_E). \tag{16}$$

Subdominant terms are obtained by higher-order contractions (e.g., setting $\mathbf{r}_2 \simeq \mathbf{r}_4$ in the second and third graphs on the right-hand side of Fig. 2). They either decay faster, or are of higher order in $\hbar_{\rm eff}$, or both. We only discuss the term that gives the long-time saturation at the ergodic value $\sigma^2(M) \simeq \hbar_{\rm eff}^2$. For $t > t_E$, there is a phase-free (and hence time-independent) contribution with four different paths, resulting from the contraction $s_1 = s_7$, $s_2 = s_8$, $s_3 = s_5$, $s_4 = s_6$, and $\mathbf{r}_1 \simeq \mathbf{r}_3$, $\mathbf{r}_2 \simeq \mathbf{r}_4$. Its contribution is sketched as the fourth diagram on the right-hand side of Fig. 2. It gives

$$\sigma_4^2 = \left(\frac{\nu^2}{\pi}\right)^{2d} \left\langle \int d\mathbf{r}_1 d\mathbf{r}_3 \sum C_{s_1} C_{s_2} \times \exp[-\nu^2(\delta\mathbf{p}_{s_1}^2 + \delta\mathbf{p}_{s_2}^2)]\Theta(\nu - |\mathbf{r}_1 - \mathbf{r}_3|)\right\rangle^2. \quad (17)$$

From the sum rule of Eq. (12), and again invoking the long-time ergodicity of the semiclassical dynamics, Eq. (15), one obtains the long-time saturation of $\sigma^2(M)$,

$$\sigma_4^2 = \hbar_{\rm eff}^2 \Theta(t - t_E). \quad (18)$$

Note that for $t < t_E$, this contribution does not exist by itself and is included in σ_1^2, Eq. (8).

According to our semiclassical approach, the fidelity has a variance given to leading order by the sum of the four terms of Eqs. (8), (13), (16), and (18)

$$\sigma_{\rm sc}^2 = \alpha^2 \exp[-2\lambda t] + 2\alpha \exp[-(\lambda + \Gamma)t] + 2\hbar_{\rm eff}\exp[-\Gamma t]\Theta(t - t_E) + \hbar_{\rm eff}^2\Theta(t - t_E). \quad (19)$$

Equation (19) is the central result of this paper. We see that for short enough times, i.e., before ergodicity and the saturation of $M(t) \simeq \hbar_{\rm eff}$ and $\sigma^2(M) \simeq \hbar_{\rm eff}^2$ is reached, the first term on the right-hand side of (19) will dominate as long as $\lambda < \Gamma$. For $\lambda > \Gamma$ on the other hand, $\sigma^2(M)$ exhibits a behavior $\propto \exp[-(\lambda+\Gamma)t]$ for $t < t_E$, turning into $\propto \hbar_{\rm eff}\exp[-\Gamma t]$ for $t > t_E$. Thus, contrary to $\overline{M}$, $\sigma^2(M)$ allows us to extract the Lyapunov exponent from the second term on the right-hand side of Eq. (19) even when $\lambda > \Gamma$. Also one sees that, unlike the strong perturbation regime $\Gamma \gg B$ [18], $M(t)$ continues to fluctuate above the residual variance $\simeq \hbar_{\rm eff}^2$ up to a time $\simeq \Gamma^{-1}|\ln \hbar_{\rm eff}|$ in the semiclassical regime $B > \Gamma > \Delta$. For $\Gamma \ll \lambda$, $\Gamma^{-1}|\ln \hbar_{\rm eff}| \gg t_E$ and $M(t)$ fluctuates beyond t_E.

The above semiclassical approach breaks down at short times for which not enough phase is accumulated to motivate a stationary phase approximation [27]. To get the short-time behavior of $\sigma^2(M)$, we instead Taylor expand the time-evolution exponentials $\exp[\pm i H_{(0)} t] = 1 \pm i H_{(0)} t - H_{(0)}^2 t^2/2 + \ldots + O(H_{(0)}^5 t^5)$. The resulting expression for $\sigma^2(M)$ contains matrix elements such as $\langle \psi_0 | H_{(0)}^a | \psi_0 \rangle$, $a = 1, 2, 3, 4$, which one then calculates using a random matrix theory (RMT) approach [26] for the chaotic quantized Hamiltonian $H_{(0)}$ [5,8,19]. Keeping nonvanishing terms of lowest order in t, one has a quartic onset $\sigma^2(M) \simeq (\overline{\Sigma^4} - \overline{\Sigma^2}^{\,2}) t^4$ for $t \ll \Sigma^{-1}$, with $\Sigma^a \equiv [\epsilon^2(\langle \psi_0 | V^2 | \psi_0 \rangle - \langle \psi_0 | V | \psi_0 \rangle^2)]^{a/2}$. RMT gives $(\overline{\Sigma^4} - \overline{\Sigma^2}^{\,2}) \propto (\Gamma B)^2$, with a system-dependent prefactor of order 1. From this and Eq. (19), one concludes that $\sigma^2(M)$ has a nonmonotonous behavior, i.e., it first rises at short times, until it decays after a time t_c, which one can evaluate by solving $\sigma_{\rm sc}^2(t_c) = (\Gamma B)^2 t_c^4$. In the regime $B > \Gamma > \lambda$ one gets

$$t_c = \left(\frac{\alpha_0}{\Gamma B}\right)^{1/2+d}\left[1 - \lambda\left(\frac{\alpha_0}{\Gamma B}\right)^{1/2+d}\frac{1}{2+d} + O\left(\lambda^2\left\{\frac{\alpha_0}{\Gamma B}\right\}^{2/2+d}\right)\right], \quad (20)$$

and thus

$$\sigma^2(t_c) \simeq (\Gamma B)^2\left(\frac{\alpha_0}{\Gamma B}\right)^{4/2+d}\left[1 - \frac{4\lambda}{2+d}\left(\frac{\alpha_0}{\Gamma B}\right)^{1/2+d} + O\left(\lambda^2\left\{\frac{\alpha_0}{\Gamma B}\right\}^{2/2+d}\right)\right]. \quad (21)$$

We explicitly took the t dependence $\alpha(t) = \alpha_0 t^{-d}$ into account. We estimate that $\alpha_0 \propto (\Gamma\lambda)^{-d/2}$ (obtained by setting the Lyapunov time equal to few times the time of flight through a correlation length of the perturbation potential, as is the case for billiards or maps), to get $\sigma^2(t_c) \propto (B/\lambda)^{2d/2+d} \gg 1$. Because $0 \leqslant M(t) \leqslant 1$, this value is, however, bounded by $\overline{M}^2(t_c)$. Since in the other regime $\Gamma \ll \lambda$, one has $\sigma^2(t_c) \simeq 2\hbar_{\rm eff}[1 - (2\hbar_{\rm eff})^{1/4}\sqrt{\Gamma/B}]$, we predict that $\sigma^2(t_c)$ grows during the crossover from $\Gamma \ll \lambda$ to $\Gamma > \lambda$, until it saturates at a non-self-averaging value, $\sigma(t_c)/\overline{M}(t_c) \approx 1$, independently on $\hbar_{\rm eff}$ and B, with possibly a weak dependence on Γ and λ.

We conclude this analytical section by mentioning that applying the RMT approach to longer times reproduces Eq. (19) with $\lambda \to \infty$ [28]. This reflects the fact that RMT is strictly recovered for $t_E = 0$ only.

To illustrate our results, we present some numerical data. We based our simulations on the kicked rotator model with Hamiltonian [29]

$$H_0 = \frac{\hat{p}^2}{2} + K_0 \cos \hat{x} \sum_n \delta(t - n). \quad (22)$$

We concentrate on the regime $K > 7$, for which the dynamics is fully chaotic with a Lyapunov exponent $\lambda = \ln[K/2]$. We quantize this Hamiltonian on a torus, which requires us to consider discrete values $p_l = 2\pi l/N$ and $x_l = 2\pi l/N$, $l = 1, \ldots N$, hence $\hbar_{\rm eff} = 1/N$. The fidelity (1) is computed for discrete times $t = n$, as

$$M(n) = |\langle \psi_0 | (U_{\delta K}^*)^n (U_0)^n | \psi_0 \rangle|^2, \quad (23)$$

using the unitary Floquet operators $U_0 = \exp[-i\hat{p}^2/2\hbar_{\rm eff}] \times \exp[-iK_0 \cos \hat{x}/\hbar_{\rm eff}]$ and $U_{\delta K}$ having a perturbed Hamiltonian H with $K = K_0 + \delta K$. The quantization procedure results in a matrix form of the Floquet operators, whose matrix elements in x representation are given by

$$(U_0)_{l,l'} = \frac{1}{\sqrt{N}} \exp\left[i\frac{\pi(l - l')^2}{N}\right] \exp\left(-i\frac{NK_0}{2\pi}\cos\frac{2\pi l'}{N}\right).$$

The local spectral density of eigenstates of $U_{\delta K}$ over those of U_0 has a Lorentzian shape with a width $\Gamma \propto (\delta K/\hbar_{\rm eff})^2$ (there is a weak dependence of Γ in K_0) in the range $B = 2\pi \gtrsim \Gamma > \Delta = 2\pi/N$). This is illustrated in the inset to Fig. 6.

Numerically, the time evolution of ψ_0 in the fidelity, Eq. (23), is calculated by recursive calls to a fast Fourier transform routine. Thanks to this algorithm, the matrix-vector multiplication $U_{0,\delta K}\psi_0$ requires $O(N \ln N)$ operations instead of $O(N^2)$, and thus allows us to deal with very large system sizes. Our data to be presented below correspond to system sizes of up to $N \leqslant 262\,144 = 2^{18}$, which still allowed us to collect enough statistics for the calculation of $\sigma^2(M)$.

We now present our numerical results. Figure 3 shows the distribution $P(M)$ of $M(t)$ in the regime $\Gamma < \lambda$ for different

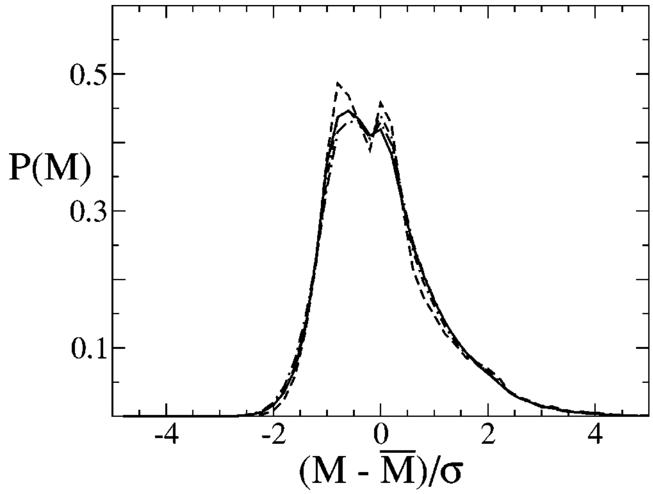

FIG. 3. Distribution $P(M)$ of the fidelity computed for 10^4 different ψ_0 for $N=32\,768$, $\delta K=5.75\times10^{-5}$ (i.e., $\Gamma\approx0.09$), at times $t=25$, 50, 75, and 100 kicks.

times. It is seen that even though $P(M)$ is not normally distributed, it is still well characterized by its variance. A calculation of $\sigma^2(M)$ is thus meaningful.

We next focus on σ^2 in the golden rule regime with $\Gamma \ll \lambda$. Data are shown in Fig. 4. One sees that $\sigma^2(M)$ first rises up to a time t_c, after which it decays. The maximal value $\sigma^2(t_c)$ in that regime increases with increasing perturbation, i.e., increasing Γ. Beyond t_c, the decay of σ^2 is very well captured by Eq. (16), once enough time has elapsed. This is due to the increase of $\sigma^2(t_c)$ above the self-averaging value $\propto\hbar_{\mathrm{eff}}$ as Γ increases. Once the influence of the peak disappears, the decay of $\sigma^2(M)$ is very well captured by σ_3^2 given in Eq. (16), without any adjustable free parameter. Finally, at large times, $\sigma^2(M)$ saturates at the value given in Eq. (18).

As δK increases, so does Γ, and $\sigma^2(M)$ decays faster and faster to its saturation value until $\Gamma \gtrsim \lambda$. Once Γ starts to exceed λ, the decay saturates at $\exp(-2\lambda t)$. This is shown in

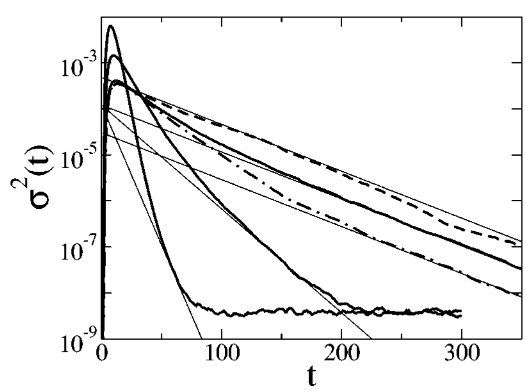

FIG. 4. Variance $\sigma^2(M)$ of the fidelity vs t for weak $\Gamma\ll\lambda$, $N=16\,384$ and $10^5\delta K=5.9$, 8.9, and 14.7 (thick solid lines), $N=4096$ and $\delta K=2.4\times10^{-4}$ (dashed line), and $N=65\,536$ and $\delta K=1.48\times10^{-5}$ (dotted-dashed line). All data have $K_0=9.95$. The thin solid lines indicate the decays$=2\hbar_{\mathrm{eff}}\exp[-\Gamma t]$, with $\Gamma=0.024(\delta KN)^2$ (there is no adjustable free parameter). The variance has been calculated from 10^3 different initial states ψ_0.

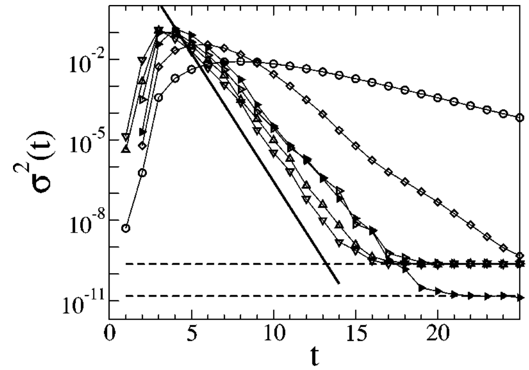

FIG. 5. Variance $\sigma^2(M)$ of the fidelity vs t in the golden rule regime with $\Gamma\gtrsim\lambda$ for $N=65\,536$, $K_0=9.95$, and $\delta K\in[3.9\times10^{-5},1.1\times10^{-3}]$ (open symbols), and $N=262\,144$, $K_0=9.95$, $\delta K=5.9\times10^{-5}$ (full triangles). The solid line is $\propto\exp[-2\lambda_1 t]$, with an exponent $\lambda_1=1.1$, smaller than the Lyapunov exponent $\lambda=1.6$, because the fidelity averages $\langle\exp[-\lambda t]\rangle$ (see text). The two dashed lines give $\hbar_{\mathrm{eff}}^2=N^{-2}$. In all cases, the variance has been calculated from 10^3 different initial states ψ_0.

Fig. 5, which corroborates the Lyapunov decay of $\sigma^2(M)$ predicted by Eqs. (8). Note that in Fig. 5, the decay exponent differs from the Lyapunov exponent $\lambda=\ln[K/2]$ due to the fact that the fidelity averages $\langle C_s\rangle\propto\langle\exp[-\lambda t]\rangle\neq\exp[-\langle\lambda\rangle t]$ over finite-time fluctuations of the Lyapunov exponent [18]. At long times, $\sigma^2(M)$ saturates at the ergodic value $\sigma^2(M,t\to\infty)=\hbar_{\mathrm{eff}}^2$, as predicted. Finally, it is seen in both Figs. 4 and 5 that t_c decreases as the perturbation is cranked up. Moreover, there is no N dependence of $\sigma^2(t_c)$ at fixed Γ. These two facts are at least in qualitative, if not quantitative, agreement with Eq. (20).

The behavior of $\sigma^2(t_c)$ as a function of Γ is finally shown in Fig. 6. First we show in the inset the behavior of the local

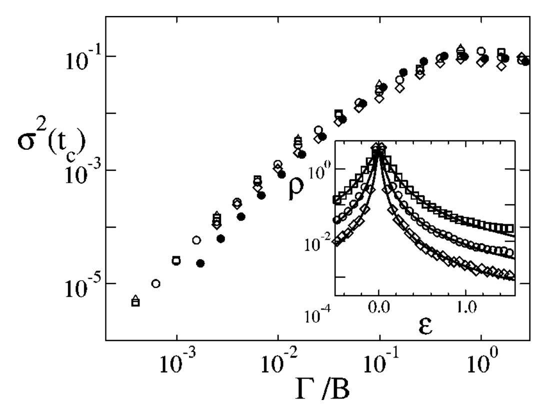

FIG. 6. Maximal variance $\sigma^2(t_c)$ as a function of Γ/B, for $K_0=10.45$, $N=4096$, $N=16\,384$, $N=65\,536$, and $N=262\,144$ (empty symbols), and $K_0=50.45$, $N=16\,384$ (full circles). The variance has been calculated from 10^3 different initial states ψ_0. Inset: the local spectral density of states $\rho(\epsilon)$ of eigenstates of an unperturbed kicked rotator with $K_0=12.56$ over the eigenstates of a perturbed kicked rotator with $K=K_0+\delta K$, $\delta K=5\times10^{-3}$. The system sizes are $N=250$ (diamonds), $N=500$ (circles), and $N=1000$ (squares). The solid lines are Lorentzian with widths $\Gamma\approx0.0125$, 0.05, and 0.0124 in agreement with the formula $\Gamma=0.024(\delta KN)^2$.

spectral density

$$\rho(\epsilon) = \sum_{\alpha} |\langle \phi_{\beta}^{(0)} | \phi_{\alpha} \rangle|^2 \delta(\epsilon - \epsilon_{\alpha} + \epsilon_{\beta}), \tag{24}$$

of eigenstates $\{\phi_{\alpha}^{(0)}\}$ (with quasienergy eigenvalues ϵ_{α}) of U_0 over the eigenstates $\{\phi_{\alpha}\}$ (with quasienergy eigenvalues $\epsilon_{\alpha}^{(0)}$) of $U_{\delta K}$. As mentioned above, $\rho(\epsilon)$ has a Lorentzian shape with a width given by $\Gamma \approx 0.024(\delta K N)^2$. Having extracted the N and δK dependence of Γ, we next plot in the main part of Fig. 6 the maximum $\sigma^2(t_c)$ of the fidelity variance as a function of the rescaled width Γ/B of $\rho(\epsilon)$. As anticipated, $\sigma^2(t_c)$ first increases with Γ until it saturates at a value $\gtrsim 0.1$, independently on $\hbar_{\text{eff}}$, Γ, or λ, once $\Gamma \approx B$. These data confirm Eq. (21) and the accompanying reasoning. Note that once Γ exceeds the bandwidth B, $\rho(\epsilon)$ is no longer Lorentzian, and the decay of both $M(t)$ and $\sigma^2(M)$ is no longer exponential [5].

In conclusion we have applied both a semiclassical and a RMT approach to calculate the variance $\sigma^2(M)$ of the fidelity $M(t)$ of Eq. (1). We found that $\sigma^2(M)$ exhibits a nonmonotonous behavior with time, first increasing algebraically, before decaying exponentially at larger times. The maximum value of $\sigma^2(M)$ is characterized by a non-self-averaging behavior when the perturbation becomes sizable against the system's Lyapunov exponent.

This work was supported by the Swiss National Science Foundation. We thank J.-P. Eckmann and P. Wittwer for discussions on structural stability, and İ. Adagideli for discussions at the early stage of this project.

[1] F. Haake, *Quantum Signatures of Chaos* (Springer, Berlin, 2000).
[2] R. Schack and C. M. Caves, Phys. Rev. Lett. **71**, 525 (1993).
[3] A. Peres, Phys. Rev. A **30**, 1610 (1984).
[4] R. A. Jalabert and H. M. Pastawski, Phys. Rev. Lett. **86**, 2490 (2001).
[5] Ph. Jacquod, P. G. Silvestrov, and C. W. J. Beenakker, Phys. Rev. E **64**, 055203(R) (2001).
[6] T. Prosen, T. H. Seligman, and M. Znidaric, Prog. Theor. Phys. Suppl. **150**, 200 (2003).
[7] N. R. Cerruti and S. Tomsovic, Phys. Rev. Lett. **88**, 054103 (2002).
[8] F. M. Cucchietti, C. H. Lewenkopf, E. R. Mucciolo, H. M. Pastawski, and R. O. Vallejos, Phys. Rev. E **65**, 046209 (2002).
[9] D. A. Wisniacki and D. Cohen, Phys. Rev. E **66**, 046209 (2002).
[10] Ph. Jacquod and D. L. Shepelyansky, Phys. Rev. Lett. **75**, 3501 (1995).
[11] J. Vanicek and E. J. Heller, Phys. Rev. E **68**, 056208 (2003).
[12] Y. Adamov, I. V. Gornyi, and A. D. Mirlin, Phys. Rev. E **67**, 056217 (2003).
[13] Ph. Jacquod, İ. Adagideli, and C. W. J. Beenakker, Europhys. Lett. **61**, 729 (2003).
[14] J. Emerson, Y. S. Weinstein, S. Lloyd, and D. G. Cory, Phys. Rev. Lett. **89**, 284102 (2002).
[15] Ph. Jacquod, İ. Adagideli, and C. W. J. Beenakker, Phys. Rev. Lett. **89**, 154103 (2002).
[16] A. Iomin, Phys. Rev. E **70**, 026206 (2004).
[17] W. Wang, G. Casati, and B. Li, Phys. Rev. E **69**, 025201(R) (2004).
[18] P. G. Silvestrov, J. Tworzydło, and C. W. J. Beenakker, Phys. Rev. E **67**, 025204(R) (2003).
[19] T. Gorin, T. Prosen, and T. H. Seligman, New J. Phys. **6**, 20 (2004).
[20] This time t^* is defined by $|\epsilon \int_0^{t^*} V(\mathbf{q}_s(t), t)| = 1$ for a typical trajectory s.
[21] P. Cvitanović, R. Artuso, R. Mainieri, G. Tanner, and G. Vattay, *Chaos: Classical and Quantum* (Niels Bohr Institute, Copenhagen 2003), www.ChaosBook.org
[22] See e.g., E. J. Heller and S. Tomsovic, Phys. Today **46**(7), 38 (1993).
[23] Setting $s = s'$ for two trajectories generated by two different Hamiltonians $H = H_0 + \epsilon V$ is justified by the structural stability of hyperbolic systems for not too large ϵ; see e.g., A. B. Katok and B. Hasselblatt, *Introduction to the Modern Theory of Dynamical Systems* (Cambridge University Press, Cambridge, 1996). In the context of the fidelity, this point was first mentioned in Ref. [11].
[24] P. Collet and J.-P. Eckmann, J. Stat. Phys. **115**, 217 (2004).
[25] G. P. Berman and G. M. Zaslavsky, Physica A **91**, 450 (1978); M. V. Berry and N. L. Balasz, J. Phys. A **12**, 625 (1979).
[26] M. L. Mehta, *Random Matrices* (Academic, New York, 1991).
[27] This time is very short, of the order of the inverse energy of the particle, i.e., $O(\hbar_{\text{eff}}^a)$, where $a \geqslant 0$ depends on the system dimension and the energy-momentum relation. For $E \propto p^2$ and in two dimensions, one has $a = 1$.
[28] C. Petitjean and Ph. Jacquod (unpublished).
[29] F. M. Izrailev, Phys. Rep. **196**, 299 (1990).